EOS

EOS, TRANSACTIONS, AMERICAN GEOPHYSICAL UNION

VOLUME 88 NUMBER 37

11 SEPTEMBER 2007

PAGES 357–368

Satellite Remote Sensing for Global Landslide Monitoring

PAGES 357–358

Rain-induced landslides rank among the most devastating natural disasters. Nearly every year worldwide they cause billions of dollars in property damage and thousands of deaths.

Society has dealt with landslide hazards primarily by trying to locate development away from known hazard zones, but such an approach has limitations. Overpopulation and associated sprawl into hazardous areas, plus environmental impacts such as deforestation and mining, increasingly put large numbers of people at risk from landslides. Yet most developing countries, particularly those in high-risk areas of the tropics, lack the data infrastructure and analysis capabilities required to minimize injuries and deaths due to landslides. The challenges facing the science community include better understanding the surface and meteorological processes that lead to landslides and determining how new technology and techniques might be applied to reduce the risk of landslides to people across the globe.

Landslide warning systems can save lives and reduce property damages if properly implemented in populated areas of landslide-prone nations [*Sidle and Ochiai*, 2006]. Such systems usually map landslide hazard zones first and then attempt to predict probabilities of landslides and associated consequences. To help with this, scientists can take advantage of advances in satellite remote sensing and other global data sets in the development of (1) global landslide susceptibility maps based on satellite-based digital elevation maps (DEM), satellite land cover information, and digital maps of soil characteristics; and (2) high time resolution, multisatellite precipitation analyses with sufficient accuracy and availability to be useful for detecting heavy rainfall events that provoke landslides.

The combination of these products potentially provides information on the "where" (susceptibility) and "when" (rain events) of landslides and the potential to detect or forecast landslide events. This article discusses the use of such information from satellite remote sensing in the study of rain-induced landslides worldwide, with an eye toward developing a system to detect or forecast such events on a global basis.

A Global Landslide Susceptibility Map

Landslide occurrence depends on complex interactions among a large number of factors, which *Dai et al.* [2002] broadly classify into two categories: (1) preparatory variables that make the land surface susceptible to slide (such as slope, soil properties, lithology, and so forth); and (2) the triggering variables that induce landmass movement (such as rainfall). The most exact method to assess landslide susceptibility is through field surveys. However, performing such surveys in data-sparse or mountainous regions is difficult; in many countries, remote sensing data may be the only information available for this purpose [*Catani et al.*, 2005; *Nadim et al.*, 2006].

Recent advances in remote sensing techniques contribute to determining landslide susceptibility by providing information on land surface features and characteristics. This global view takes advantage of high-resolution DEM data from the NASA Shuttle Radar Topography Mission (SRTM; http://www2.jpl.nasa.gov/srtm/). The SRTM data, which can resolve features up to 30 meters

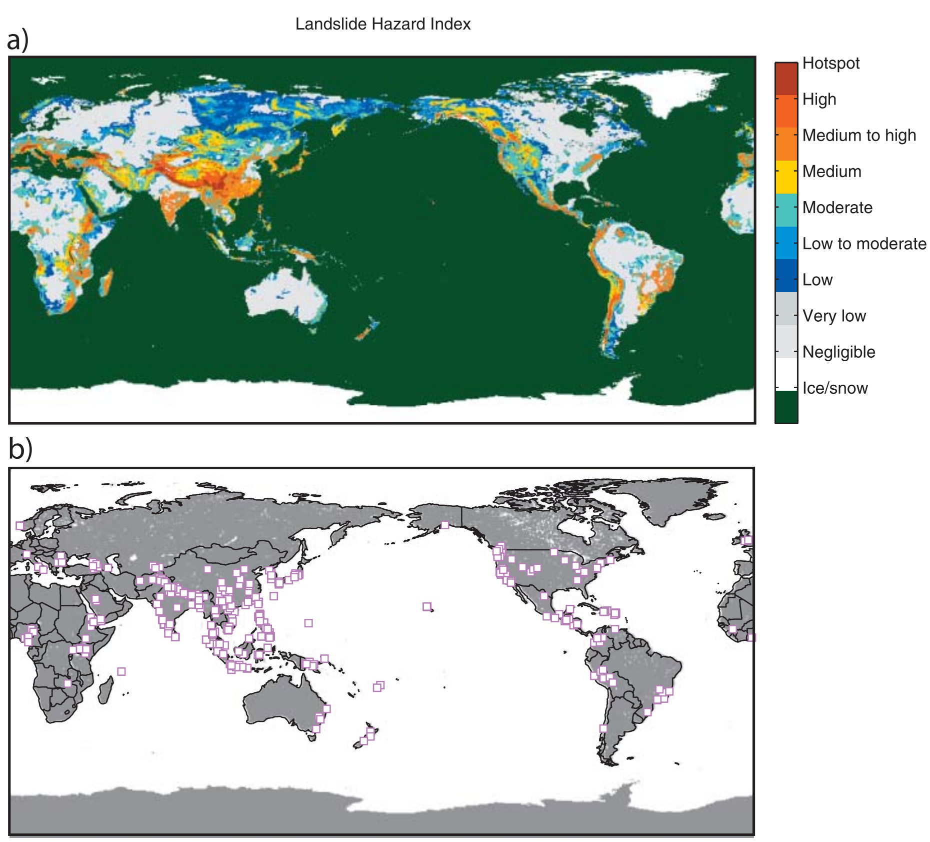

Figure 1 (a) Global landslide hazard index and hot spots and (b) landslide occurrences collected from news reports and other sources during the period of January 2004 through September 2006. Note how the actual landslides in Figure 1b match with regions identified as having high landslide susceptibility.

BY Y. HONG, R. F. ADLER, AND G. J. HUFFMAN

in size, are used to derive topographic factors (slope, orientation, and so forth) and provide a major breakthrough in digital elevation mapping of the world. In addition, digital maps of soil characteristics prepared by the Food and Agriculture Organization of the United Nations (http://www.fao.org/AG/agl/agll/dsmw.htm) and satellite-based land cover information (e.g., from NASA's Moderate Resolution Imaging Spectroradiometer (MODIS; http://modis.gsfc.nasa.gov)) are combined with information from the SRTM to estimate a static landslide susceptibility index for each point on the globe over land. The satellite precipitation information in this study includes the Tropical Rainfall Measuring Mission (TRMM) Multi-satellite Precipitation Analysis (TMPA [*Huffman et al.*, 2007]; http://trmm.gsfc.nasa.gov).

As needed, the various land data sets are downscaled by linear interpolation to spatially match the SRTM data in order to estimate hazards at the finest resolution. A global landslide susceptibility map is then derived following *Hong et al.* [2007a] from these geospatial data based on different factors' relative significance to the sliding processes. These factors primarily include slope and lithology with land cover type and soil properties having secondary importance.

Figure 1a shows the resulting global Landslide Susceptibility Index (LSI) map with a descriptive scale ranging from "negligible" to "high." Excluding permanent snow or ice regions, Figure 1a shows that the low LSI areas cover about half of the land (52%) while the areas of high LSI (4%) are mostly located in tropical or subtropical regions. The typical high LSI regions are the Pacific Rim, the Himalayan belt, South Asia, Southeast Asia and surrounding islands, Central America, northwestern United States and Canada, the Rocky Mountains, the Appalachian Mountains, the Caucasus region, the Alps, and parts of the Middle East and Africa.

Figure 1b shows the spatial distribution of major landslide occurrences collected from news reports and other sources during the period of January 2004 through September 2006. The distribution of landslide occurrences in Figure 1b generally confirms the regions identified by the derived LSI map.

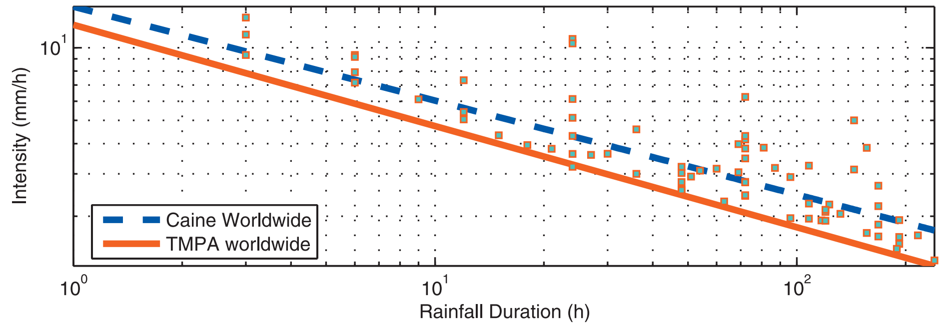

Fig. 2. Satellite-based rainfall intensity-duration threshold curve for triggering landslides (orange line) for landslides (squares) that occurred around the globe in the period 1998–2005; and rain-gauge-based threshold (dashed blue line) curve from Caine *[1980; after* Hong et al.*, 2006]. Note that the satellite-based threshold falls below Caine's threshold, likely because the satellite rainfall is an area-average value, rather than a point accumulation.*

Rainfall and Landslides

The spatial distribution, duration, and intensity of precipitation play important roles in triggering landslides. Comprehensive modeling of the physical processes involved in landslides helps pinpoint causes of landmass movement [*Keefer and Wilson*, 1987; *Iverson et al.*, 2000] in relation to rainfall. However, data requirements for implementing such models can often be prohibitive. For practical purposes, the process is often simplified [*Gritzner et al.*, 2001].

In practice, landslide occurrence has been related empirically to rainfall intensity-duration statistics from rain gauge information for specific regions [*Larsen and Simon*, 1993; *Godt et al.*, 2006] and on a quasi-global basis [*Caine*, 1980]. The recent development of high time resolution, multisatellite precipitation analyses has provided the potential of detecting heavy rain events associated with landslides in tropical and temperate latitudes without regard for the availability of rain gauges, an issue that frequently limits the application of the previous studies. By using the precipitation information from TMPA, *Hong et al.* [2006] derived the first satellite-based rainfall intensity-duration threshold curve from landslide cases in various climate and geological locations and compared it with similar curves from the previous rain-gauge-based studies (Figure 2). Note that the TMPA-based threshold falls below Caine's threshold, likely because the TMPA is an area-average value, rather than a point accumulation.

Landslide Prediction

Knowledge of landslide susceptibility as displayed in Figure 1 (the "where" of the problem) and the ability to detect heavy rain events that meet threshold conditions as shown in Figure 2 (the "when" of the problem) provide the basis for exploring the potential and limitations of such approaches for analyzing and studying the occurrences of landslides, and even possibly forecasting them.

A preliminary evaluation using the information in Figures 1 and 2 demonstrates the potential effectiveness of this approach, at least for 25 large events examined by *Hong et al.* [2007b]. Taking the landslide cases in Figure 2 and keeping only the ones with greater than moderate susceptibility in Figure 1, the probability of detection is 0.76, which is equal to 19 successful detections out of 25 occurrences. However, the results also indicate that this first-generation system fails to identify landslides triggered by short-duration heavy rainfall events (<6 hours) or by rain falling on snow, as melting snow can sometimes trigger landslides.

These early studies are merely a starting point, and improvements are expected in the analysis system as well as in satellite data retrievals for both the land surface and rainfall information. The authors judge that landslide forecasts will likely be limited to estimating areas (scale of approximately 25–100 kilometers) with a high probability of a landslide occurring in that region during a period of a few days. Detailed retrospective analysis of probability of detection and false alarm rate will be required to determine the potential for warning. The 9 years (and continuing) of TMPA rainfall data record will be key to this study.

In the future, the increasing availability of improved yet low-cost remote sensing products that can support geographic information system (GIS)–based landslide models will likely be useful for disaster prevention for landslide-prone regions. In order to issue landslide warning forecasts, more accurate medium-range rainfall forecasts will be required to foresee the probability of a landslide occurring in high susceptibility regions at lead times of several days. Prior to achieving that, the challenge facing the research community is to continue to develop techniques to better understand landslide processes that translate into potential warning applications. Such efforts must be practical with respect to local expertise and facilities available. The development should also involve capacity-building for the vulnerable countries so that they can take advantage of the technical advances. To achieve this, several things should be emphasized:

- improved, high-resolution representation of land surface and subsurface characteristics from remote sensing techniques and field surveys,
- establishment of a global landslide inventory database that includes causes, physical measurements, process descriptions, and socioeconomic impacts,
- better understanding and modeling of the landslide processes, and
- interdisciplinary efforts and multination collaboration.

Further work is needed to implement these concepts into a cost-effective method for landslide risk management in developing countries.

Acknowledgement

This work is supported by NASA's Applied Science Program under Stephen Ambrose of NASA Headquarters.

References

Caine, N. (1980), The rainfall intensity-duration control of shallow landslides and debris flows, *Geogr. Ann., Ser. A, 62*, 23–27.
Catani, F., N. Casagli, L. Ermini, G. Righini, and G. Menduni (2005), Landslide hazard and risk mapping at catchment scale in the Arno River basin, *Landslide, 2*(4), 329–342, doi:10.1007/s10346-005-0021-0.
Dai, E. C., C. F. Lee, and Y. Y. Nagi (2002), Landslide risk assessment and management: An overview, *Eng. Geol., 64*, 65–87.
Godt, J. W., R. L. Baum, and A. F. Chleborad (2006), Rainfall characteristics for shallow landsliding in Seattle, Washington, USA, *Earth Surf. Processes Landforms, 31*, 97–110.
Gritzner, M. L., W. Marcus, R. Aspinall, and S. Custer (2001), Assessing landslide potential using GIS, soil wetness modeling and topographic attributes, Payette River, Idaho, *Geomorphology, 37*, 149–165.
Hong, Y., R. Adler, and G. Huffman (2006), Evaluation of the potential of NASA multi-satellite precipitation analysis in global landslide hazard assessment, *Geophys. Res. Letter, 33*, L22402, doi:10.1029/2006GL028010.
Hong, Y., R. Adler, and G. Huffman (2007a), Use of satellite remote sensing data in mapping of global shallow landslide susceptibility, *J. Nat. Hazards, 43*(2), doi:10.1007/s11069-006-9104-z.
Hong, Y., R. Adler, and G. Huffman (2007b), An experimental global prediction system for rainfall-triggered landslides using satellite remote sensing and geospatial datasets, *IEEE Trans. Geosci. Remote Sens., 45*(6), 1671–1680, doi:10.1109/TGRS.2006.888436.
Huffman, G. J., R. F. Adler, D. T. Bolvin, G. Gu, E. J. Nelkin, K. P. Bowman, Y. Hong, E. F. Stocker, and D. B. Wolff (2007), The TRMM multi-satellite precipitation analysis: Quasi-global, multi-year, combined-sensor precipitation estimates at fine scale, *J. Hydrometeorol., 8* (1), 38–55.
Iverson, R. M., M. E. Reid, N. R. Iverson, R. G. LaHusen, M. Logan, J. E. Mann, and D. L. Brien (2000), Acute sensitivity of landslide rates to initial soil porosity, *Science, 290*, 20.
Keefer, D. K., and R. C. Wilson (1987), Real-time landslide warning during heavy rainfall, *Science, 238*(13), 921–925.
Larsen, M. C., and A. Simon (1993), A rainfall intensity-duration threshold for landslides in a humid-tropical environment, Puerto Rico, *Geogr. Ann., 75*, 13–23.
Nadim, F., O. Kjekstad, P. Peduzzi, C. Herold, and C. Jaedicke (2006), Global landslide and avalanche hotspots, *J. Landslides, 3*(2), 159–173, doi:10.1007/s10346-006-0036-1.
Sidle, R. C., and H. Ochiai (2006), *Landslides: Processes, Prediction, and Land Use, Water Resour. Monogr. Ser.*, vol. 18, 312 pp., AGU, Washington, D. C.

Author Information

Yang Hong, Laboratory for Atmospheres, NASA Goddard Space Flight Center, Greenbelt, Md.; now at School of Civil Engineering and Environmental Sciences, University of Oklahoma, Norman; E-mail: yanghong@agnes.gsfc.nasa.gov; Robert F. Adler, Laboratory for Atmospheres, NASA Goddard Space Flight Center; and George J. Huffman, Laboratory for Atmospheres, NASA Goddard Space Flight Center; also at Science Systems and Applications, Inc., Lanham, Md.

Overview of Midlatitude Ionospheric Storms

PAGES 358–359

Solar flares and coronal mass ejections erupting from the roiling Sun can smash into the Earth's magnetosphere causing geomagnetic storms that penetrate deep into the atmosphere, which can short out satellites, upset radio communications, disrupt navigation, and even damage terrestrial electrical power grids. Though effects on other regions of the atmosphere have been analyzed, the mechanism by which geomagnetic storms influence the ionosphere's middle latitudes remains poorly understood.

This brief report provides an overview of current knowledge in midlatitude ionospheric dynamics and disturbances, from the historic record to recent discoveries presented at a January AGU Chapman Conference.

Geomagnetic Storms and the Midlatitude Ionosphere

Recent discoveries demonstrate that during geomagnetic storms the ionosphere rises up, thickens, and accelerates over regions extending nearly 90° in latitude, leading to the poleward movement of huge volumes of plasma. The plasma and its movement are produced by impulses of electric field from the solar wind and surges of thermospheric winds. Further, sharp gradients in ionospheric content extending thousands of kilometers are created by unknown factors [*Foster and Rideout*, 2005]. These gradients spawn irregularities that create disturbances in radio transmissions [*Ledvina et al.*, 2002]. At higher altitudes the dramatic changes in the ionosphere are associated with transport in the plasmasphere, a region of extended thermal plasma on closed field lines.

Within this system, at midlatitudes the ionosphere experiences extreme changes. The midlatitude ionosphere was first studied during the "discovery era" of radio physics and spaceflight 50 or more years ago, but for the past three decades the polar and tropical ionosphere has dominated scientific activity. This left the false impression that the midlatitude ionosphere was an uninteresting region of known morphology and well-understood processes.

During the past 5 years, the ability to image the ionosphere and thermosphere with large networks of ground-based GPS receivers and satellite-borne GPS receivers dramatically changed this viewpoint. Studies with these new data quickly revealed that the most extreme examples of ionospheric volume, total electron content (TEC), occur at midlatitudes during geomagnetic storms. There, TEC can change by factors of 3–10 over the duration of a magnetic storm [*Tsuratani et al.*, 2005].

The midlatitude ionosphere is driven by two largely unconstrained mechanisms: the inner magnetospheric electric field originating in the heliosphere, and the dynamic and electrodynamic properties of the thermosphere. This past January, the Chapman Conference on Mid-latitude Ionospheric Dynamics and Disturbances, or MIDD, brought together three communities to investigate this control: the ionospheric community, which is characterizing the midlatitude domain; the magnetospheric and solar wind community, which is investigating how inner magnetospheric electric fields map to and transport the midlatitude ionosphere; and the thermospheric community, which is investigating how neutral winds and composition control the midlatitude ionosphere.

During geomagnetic storms, electric fields and neutral winds are strongly driven, yielding ionospheric space weather in the form of gradients and irregularities in the ionospheric density. When these fields and winds occur at midlatitudes, the effects of ionospheric space weather take on special importance, particularly in how they potentially disrupt GPS signals [*Walter et al.*, 2004]. Because of this vulnerability, midlatitude ionospheric storms must be better understood.

Characterizing Midlatitude Ionospheric Storms

Determining what defines a midlatitude ionospheric storm is controversial and revolves around whether equatorial or high-latitude dynamics move to midlatitudes or whether another combination of geophysical processes is at work. Historically, midlatitude ionospheric storms are described as having a positive phase in which plasma density increases early during a geomagnetic storm, and a negative phase in which plasma density decreases during the recovery phase of a geomagnetic storm. However, incoherent scatter radar measurements have demonstrated that the positive phase can be highly structured with phenomena such as subauroral polarization streams, storm-enhanced densities, and subauroral ion drifts.

In recent years, networks of GPS receivers yielding TEC measurements have made possible continent-sized images of the North American ionosphere. In these images, large volumes of plasma are created during daylight as the Sun ionizes the upper atmosphere, and flow poleward across the